

Multi-Kink Quantile Regression for Longitudinal Data with Application to the Progesterone Data Analysis

Chuang Wan¹, Wei Zhong^{1,*}, Wenyang Zhang³ and Changliang Zou⁴

¹ Xiamen University; ²The University of York; ³ Nankai University

*Email: wzhong@xmu.edu.cn

First version: December 20, 2020

December 10, 2021

Abstract

Motivated by investigating the relationship between progesterone and the days in a menstrual cycle in a longitudinal study, we propose a multi-kink quantile regression model for longitudinal data analysis. It relaxes the linearity condition and assumes different regression forms in different regions of the domain of the threshold covariate. In this paper, we first propose a multi-kink quantile regression for longitudinal data. Two estimation procedures are proposed to estimate the regression coefficients and the kink points locations: one is a computationally efficient profile estimator under the working independence framework while the other one considers the within-subject correlations by using the unbiased generalized estimation equation approach. The selection consistency of the number of kink points and the asymptotic normality of two proposed estimators are established. Secondly, we construct a rank score test based on partial subgradients for the existence of kink effect in longitudinal studies. Both the null distribution and the local alternative distribution of the test statistic have been derived. Simulation studies show that the proposed methods have excellent finite sample performance. In the application to the longitudinal progesterone data, we identify two kink points in the progesterone curves over different quantiles and observe that the progesterone level remains stable before the day of ovulation, then increases quickly in five to six days after ovulation and then changes to stable again or even drops slightly.

Keywords: Longitudinal data analysis; multi-kink; progesterone data; quantile regression; efficiency; score test.

1 Introduction

Longitudinal data are frequently observed in many fields such as clinical medicine, biomedical science, social sciences and economics. In longitudinal data, the within-subject correlations of repeated measurements bring many challenges to both parameter estimation and statistical inference. In traditional regression analysis such as linear regression, the impacts of covariates on a response are often assumed to be constant on the whole domain of the covariates. However, this assumption may be invalid in some applications. Li et al. (2015) developed the bent line quantile regression (Li et al., 2011) for the longitudinal framework and showed that the cognitive decline was gradual like normal aging in the preclinical stage of Alzheimer’s disease (AD) and then distinguishably accelerated as the disease progresses after a certain change point. The bent line regression (Li et al., 2011) or the kink regression (Hansen, 2017) assumes that different regression forms are separately modeled on two sides of an unknown threshold but still continuous at the threshold. Li and Zhang (2011) also found that there exists a threshold effect between the blood pressure change and the progression of microalbuminuria among individuals with type-I diabetes using censored longitudinal data. Ge et al. (2020) proposed a threshold linear mixed model to determine the cutpoint of a continuous regressor and to estimate the interaction effect between the treatment and subgroup indicator on longitudinal responses.

All these aforementioned methods assume there is only one single change point. This assumption could not be satisfied in applications. Without prior knowledge on the single kink point assumption, it is more reasonable to assume a general regression model with multiple kink points for the longitudinal data. Das et al. (2016) introduced a likelihood-based estimation approach for a broken-stick model with multiple change points for longitudinal data. However, the number of change points is assumed to be known as a priori. Zhong et al. (2021) considered a multi-kink quantile regression for the independent data. However, the model does not directly apply to longitudinal data. As Li et al. (2015) mentioned, “*Extensions to handle two or more change-points in the model are prohibited by algorithmic issues and merit future research.*” This motivates us to study the multi-kink quantile regression (MKQR) for longitudinal data analysis.

In this paper, we propose a multi-kink quantile regression (MKQR) model for longitudinal data. It assumes different regression forms in different regions of the domain of the threshold

covariate. The multi-kink regression can be considered as a special case of partial linear regression where the nonlinear relationship between the response and the threshold covariate is captured by a continuous piecewise linear model. Compared with nonparametric models, such as spline regression, the multi-kink design has the better interpretability by detecting the kink points locations and maintaining linear regressions in each segment of the threshold covariate. We summarize main contributions as follows. First, the MKQR model allows the covariate effects and kink points to vary across different quantiles and is robust to outliers and heavy-tailed errors simultaneously. Two estimation procedures are proposed to estimate the regression coefficients and the kink points. One is a computationally efficient two-step estimation procedure under the working independence framework where the within-subject correlations are ignored in the estimation step. The other one is a generalized estimating equation (GEE) estimator (Liang and Zeger, 1986) to incorporate the correlation information within subjects. We estimate the number of kink points by transforming it into a model selection problem based on a quantile information criterion. The selection consistency of the number of kink points and the asymptotic normality of the estimators are established. Second, we construct a rank score test based on partial subgradients for the existence of kink effect at a given quantile level for longitudinal data analysis. Both the null distribution and the local alternative distribution of the test statistic have been theoretically studied. Third, we apply the proposed MKQR model to the longitudinal progesterone data to clearly identify two distinguishable kink points in the progesterone curves over different quantiles. We observe that the progesterone level remains stable before the day of ovulation, then increases quickly in five to six days after ovulation and then changes to stable again or even drops slightly after the second kink point. Last, new R functions for longitudinal data analysis are developed in the R package *MultiKink* to implement the proposed estimation and inference procedures.

The rest of this paper is organized as follows. In Section 2, we introduce the multi-kink quantile regression for the longitudinal data and two parameter estimation procedures. The asymptotic properties are studied in Section 3. Section 4 presents a quantile score-type test for the existence of kink points. Intensive simulation studies are conducted in Section 5 to evaluate the finite sample performances of the proposed methods. The longitudinal progesterone data analysis is included in Section 6. A concluding remark is given in Section 7. The technical proofs and additional simulation results are provided in the Appendix.

2 Model and Methodologies

2.1 Model setting

Let Y_{ij} denote a response of interest, X_{ij} be a univariate threshold variable and \mathbf{Z}_{ij} be a p -dimensional additional covariates at the j th observation for the i th subject, where $j = 1, 2, \dots, n_i$ and $i = 1, 2, \dots, N$. Let $n = \sum_{i=1}^N n_i$ be the total number of observations. Denote $\mathbf{W}_{ij} = (X_{ij}, \mathbf{Z}_{ij}^T)^T$. Without loss of generality, we assume X_{ij} has a bounded support set $[M_1, M_2]$. At a given quantile level $\tau \in (0, 1)$, define the τ th condition quantile of Y given \mathbf{W} as $Q_Y(\tau|\mathbf{W}) = F^{-1}(\tau|\mathbf{W}) = \inf\{u : F(u|\mathbf{W}) \geq \tau\}$, where $F(\cdot|\mathbf{W})$ is the conditional density of Y given \mathbf{W} .

We consider a more flexible multi-kink quantile regression (MKQR) with an undetermined number of kink points for the longitudinal data,

$$Y_{ij} = \alpha_{0,\tau,0} + \alpha_{1,\tau,0}X_{ij} + \sum_{k=1}^{K_0} \beta_{k,\tau,0}(X_{ij} - t_{k,\tau,0})I(X_{ij} > t_{k,\tau,0}) + \mathbf{Z}_{ij}^T \boldsymbol{\gamma}_{\tau,0} + e_{ij}^{(\tau)}, \quad (2.1)$$

where $M_1 < t_{1,\tau} < t_{2,\tau} < \dots < t_{K_0,\tau} < M_2$ are K_0 kink points and $\beta_{k,\tau,0} \neq 0$ for $k = 1, \dots, K_0$ is the difference in slopes for the adjacent k th and $(k+1)$ th regimes. There are totally $K_0 + 1$ regimes divided by K_0 kink points. $e_{ij}^{(\tau)}$ is the error term with the τ th quantile being zero conditional on X_{ij} and \mathbf{Z}_{ij} . In the longitudinal models, $e_{ij}^{(\tau)}$'s are usually independent across subjects but correlated within a subject. It is worth emphasizing that although the slope of X_{ij} is discontinuous at t_τ , but the regression function is continuous everywhere on the whole domain of X .

Denote $\boldsymbol{\eta}_0(\tau) = (\alpha_{0,\tau,0}, \alpha_{1,\tau,0}, \beta_{1,\tau,0}, \dots, \beta_{K_0,\tau,0}, \boldsymbol{\gamma}_{\tau,0}^T)^T$ as the vector of the true regression coefficients and $\mathbf{t}_0(\tau) = (t_{1,\tau,0}, \dots, t_{K_0,\tau,0})^T$ as the vector of true kink points. Although all parameters including K_0 depends on the quantile level τ , we will suppress such dependence on τ for ease of notations. Model (2.1) can be re-expressed as the conditional quantile form

$$Q_Y(\tau; \boldsymbol{\theta}_0 | \mathbf{W}_{ij}) = \alpha_{0,0} + \alpha_{1,0}X_{ij} + \sum_{k=1}^{K_0} \beta_{k,0}(X_{ij} - t_{k,0})_+ + \mathbf{Z}_{ij}^T \boldsymbol{\gamma}_0, \quad (2.2)$$

where $\boldsymbol{\theta}_0 = (\boldsymbol{\eta}_0^T, \mathbf{t}_0^T)^T$ and $(a)_+ = aI(a > 0)$ for any $a \in \mathbb{R}$. As pointed by Li et al. (2015), model (2.2) means that 100 τ % of the subjects have an outcome value no longer than $\alpha_{0,0} + \alpha_{1,0}X_{ij} + \sum_{k=1}^{K_0} \beta_{k,0}(X_{ij} - t_{k,0})_+ + \mathbf{Z}_{ij}^T \boldsymbol{\gamma}_0$.

2.2 Parameter estimation

We first introduce two estimation procedures to estimate the regression coefficients and the kink points given a fixed number of kink points. Then, we estimate the true number of kink points using a model selection approach based on a quantile information criterion.

2.2.1 A working independence framework

To estimate $\boldsymbol{\theta} = (\boldsymbol{\eta}^\top, \mathbf{t}^\top)^\top$, a computationally efficient way is to ignore possible correlations among measurements within subjects and to minimize the following objective function

$$S_n(\boldsymbol{\theta}) = n^{-1} \sum_{i=1}^N \sum_{j=1}^{n_i} \rho_\tau\{Y_{ij} - Q_Y(\tau; \boldsymbol{\theta} | \mathbf{W}_{ij})\}, \quad (2.3)$$

where $n = \sum_{i=1}^N n_i$ is the total number of all observations and $\rho_\tau(v) = v\{\tau - I(v < 0)\}$ is the quantile check function. It is not easy to directly minimize (2.3) since the objective function is neither differentiable nor convex. To this end, we propose a two-step profile estimation strategy to estimate both regression coefficients and kink location parameters simultaneously. The estimation steps are listed as below.

- **Step 1:** Given a fixed number of kink points K , the dimension of $\boldsymbol{\theta}$ is also determined. The profile estimator of $\boldsymbol{\eta}$ conditional on \mathbf{t} is obtained by

$$\hat{\boldsymbol{\eta}}^I(\mathbf{t}) = \arg \min_{\boldsymbol{\eta} \in \mathcal{B}} S_n(\boldsymbol{\eta}, \mathbf{t}), \quad (2.4)$$

where $\mathcal{B} \subset \mathbb{R}^{2+p+K}$ is a compact set for $\boldsymbol{\eta}$.

- **Step 2:** The estimator for \mathbf{t} at a given K is therefore defined as

$$\hat{\mathbf{t}}^I = \arg \min_{\mathbf{t} \in \boldsymbol{\Lambda}} S_n\left\{\hat{\boldsymbol{\eta}}^I(\mathbf{t}), \mathbf{t}\right\} \quad (2.5)$$

where $\boldsymbol{\Lambda} = (M_1 + \epsilon \leq t_1 < t_2 < \cdots < t_K \leq M_2 - \epsilon)$ is a constrained region for \mathbf{t} and ϵ is a small positive number to avoid edge effect. Minimization of (2.5) is a linearly constrained optimization which can be implemented by the adaptive barrier algorithm.

The two-step profile estimation procedure with ignoring the within-subject correlations is computationally efficient even when K is relatively large. We denote the estimators under the working independence framework as $\hat{\boldsymbol{\theta}}^I = \left(\hat{\boldsymbol{\eta}}^{I^\top}(\hat{\mathbf{t}}^I), \hat{\mathbf{t}}^{I^\top}\right)^\top$.

2.2.2 Incorporating correlations by using GEE

Since the ignored within-subject correlations may incur some estimation efficiency loss, we then consider an efficient generalized estimating equation (GEE) approach (Liang and Zeger, 1986) to incorporate the within-subject correlations of longitudinal data. We estimate $\boldsymbol{\theta}$ through the estimating equation

$$\sum_{i=1}^N \mathcal{X}_i(\boldsymbol{\theta}) \mathbf{A}_i^{-1} \psi_\tau\{\mathbf{Y}_i - \mathbf{Q}_i(\tau; \boldsymbol{\theta} | \mathbf{W}_i)\} = \mathbf{0}, \quad (2.6)$$

where $\mathbf{Y}_i = (Y_{i1}, \dots, Y_{in_i})^\top$, $\mathcal{X}_i(\boldsymbol{\theta}) = (\mathcal{X}_{i1}(\boldsymbol{\theta}), \dots, \mathcal{X}_{in_i}(\boldsymbol{\theta}))^\top$ with $\mathcal{X}_{ij}(\boldsymbol{\theta}) = (1, X_{ij}, (X_{ij} - t_1)_+, \dots, (X_{ij} - t_K)_+, \mathbf{Z}_{ij}^\top, -\beta_1 I(X_{ij} > t_1), \dots, -\beta_K I(X_{ij} > t_K))^\top$, $\psi_\tau(u) = \tau - I(u < 0)$, $\psi_\tau(\mathbf{u}_i) = (\psi_\tau(u_{i1}), \dots, \psi_\tau(u_{in_i}))^\top$ and $\mathbf{Q}_i(\tau; \boldsymbol{\theta} | \mathbf{W}_i) = (Q_Y(\tau; \boldsymbol{\theta} | \mathbf{W}_{i1}), \dots, Q_Y(\tau; \boldsymbol{\theta} | \mathbf{W}_{in_i}))^\top$. \mathbf{A}_i is an $n_i \times n_i$ working correlation matrix to account for the correlations among observations within the i th subject. However, the efficiency of the GEE method relies on the correct specification of \mathbf{A}_i , and it will loss the estimation efficiency once \mathbf{A}_i is misspecified. To overcome this issue, we apply the quadratic inference functions (QIF) method (Qu et al., 2000) to characterize \mathbf{A}_i by a linear combination of basic matrices using

$$\mathbf{A}_i^{-1} = \sum_{l=1}^v a_l \mathbf{M}_{li},$$

where \mathbf{M}_{li} is some given basic matrices, a_l 's are unknown constants, $l = 1, \dots, v$. As pointed by Qu et al. (2000), the basic matrices family should be rich enough to accommodate or at least approach the true correlation structures. For example, if the working correlation has the AR(1) structure, then \mathbf{A}_i^{-1} can be represented by a combination of three basis matrices \mathbf{M}_{1i} , \mathbf{M}_{2i} and \mathbf{M}_{3i} , where \mathbf{M}_{1i} is the identity matrix, \mathbf{M}_{2i} has 1 on the two main subdiagonals and 0 elsewhere, and \mathbf{M}_{3i} has 1 on (1,1) and (n_i, n_i) components and 0 elsewhere.

In the QIF approach, we do not need to directly estimate the nuisance parameters a_l 's to explicitly specify the correlation structure. Instead, we consider multiple sets of estimating equations based on basic matrices to estimate $\boldsymbol{\theta}$, for $l = 1, \dots, v$,

$$\sum_{i=1}^N \mathbf{S}_{il}(\boldsymbol{\theta}) = \sum_{i=1}^N \mathcal{X}_i(\boldsymbol{\theta})^\top \mathbf{M}_{li} \psi_\tau\{\mathbf{Y}_i - \mathbf{Q}_i(\tau; \boldsymbol{\theta} | \mathbf{W}_i)\} = 0. \quad (2.7)$$

Since the number of estimation equations is greater than the number of parameters, we apply the idea of the generalized method of moments (GMM) (Hansen, 1982) to estimate $\boldsymbol{\theta}$

by combining multiple sets of estimating equations,

$$\widehat{\boldsymbol{\theta}}^C = \arg \min_{\boldsymbol{\theta}} \mathbf{P}_N(\boldsymbol{\theta}) \equiv \arg \min_{\boldsymbol{\theta}} \mathbf{S}(\boldsymbol{\theta}) \boldsymbol{\Xi}_N^{-1}(\boldsymbol{\theta}) \mathbf{S}(\boldsymbol{\theta}), \quad (2.8)$$

where $\mathbf{S}(\boldsymbol{\theta}) = N^{-1} \sum_{i=1}^N \mathbf{S}_i(\boldsymbol{\theta})$ with $\mathbf{S}_i(\boldsymbol{\theta}) = (\mathbf{S}_{i1}^T(\boldsymbol{\theta}), \dots, \mathbf{S}_{iw}^T(\boldsymbol{\theta}))^T$, and $\boldsymbol{\Xi}_N(\boldsymbol{\theta})$ is the covariance matrix of $\mathbf{S}_i(\boldsymbol{\theta})$ which can be estimated by $N^{-1} \sum_{i=1}^N \mathbf{S}_i(\boldsymbol{\theta}) \mathbf{S}_i^T(\boldsymbol{\theta}) - \mathbf{S}(\boldsymbol{\theta}) \mathbf{S}^T(\boldsymbol{\theta})$. From the computational aspect, we apply the induced smoothing technique in Leng and Zhang (2014) for (2.8) and solve the smoothed objective function using the Newton-Raphson method. The detailed algorithm and the asymptotical equivalence are included in the Web Appendix A.

2.3 Determine the number of kink points

In real data analysis, the true number of kink points is usually unknown in practice and needs to be identified. In this subsection, we consider a model selection procedure to consistently estimate the true number of kink points. With slight abuse of notation, we impose the subscript “ k ” for parameter vectors to emphasize the MKQR model with k kink points in the estimation parts. By letting $k = 0, 1, \dots, K^*$, we can obtain $K^* + 1$ candidate models estimation results by using previous estimation procedures, where K^* is a pre-specified maximum number of kink points. Selecting an optimal K can be transformed to a model selection problem. We consider the Schwarz-type quantile information criterion:

$$\text{SIC}(k) = \log \left\{ S_n(\widehat{\boldsymbol{\theta}}_k) \right\} + \frac{\log(n)}{2n} \omega_k, \quad (2.9)$$

where $\widehat{\boldsymbol{\theta}}_k$ is the estimates for $\boldsymbol{\theta}_k$ using one of two estimation procedures, and $\omega_k = 2 + p + 2k$ is the length of parameter vectors. Thus, the estimator for K is $\widehat{K} = \arg \min_{k=0,1,\dots,K^*} \text{SIC}(k)$. Once K is determined, the final estimator for $\boldsymbol{\theta}$ is also obtained consequently.

3 Asymptotic Properties

3.1 Asymptotic Normality

We first study the limiting distribution of the profile estimator $\widehat{\boldsymbol{\theta}}^I$ under the working independence framework. Define the following two matrices:

$$\mathbf{H}_n = n^{-1} \sum_{i=1}^N \sum_{j=1}^{n_i} f_{ij} \{Q_Y(\tau; \boldsymbol{\theta}_0 | \mathbf{W}_{ij})\} \mathcal{X}_{ij}(\boldsymbol{\theta}_0) \mathcal{X}_{ij}(\boldsymbol{\theta}_0)^T,$$

where $f_{ij} \{Q_Y(\tau; \boldsymbol{\theta}_0 | \mathbf{W}_{ij})\}$ is the conditional density function of Y_{ij} given \mathbf{W}_{ij} ; and

$$\boldsymbol{\Sigma}_n(\boldsymbol{\delta}) = n^{-1} \left\{ \sum_{i=1}^N \sum_{j=1}^{n_i} \tau(1-\tau) \mathcal{X}_{ij}(\boldsymbol{\theta}_0) \mathcal{X}_{ij}(\boldsymbol{\theta}_0)^T + \sum_{i=1}^N \sum_{j \neq j'}^{n_i} (\delta_{ijj'} - \tau^2) \mathcal{X}_{ij}(\boldsymbol{\theta}_0) \mathcal{X}_{ij'}(\boldsymbol{\theta}_0)^T \right\},$$

where $\delta_{ijj'} - \tau^2$ is aroused by $Cov\{\psi_\tau(e_{ij}), \psi_\tau(e_{ij'})\}$, $\delta_{ijj'} = P(e_{ij} < 0, e_{ij'} < 0)$ measures the dependence of residuals across different measurements from the same subject and $\boldsymbol{\delta} = (\delta_{ijj'}; i = 1, \dots, N, j, j' = 1, \dots, n_i)^T$.

Theorem 3.1. *Under Assumptions (A1)-(A6) in the Web Appendix A, then under Model (2.2), $\widehat{\boldsymbol{\theta}}^I$ is \sqrt{n} -consistent and asymptotically normal, that is*

$$\sqrt{n}(\widehat{\boldsymbol{\theta}}^I - \boldsymbol{\theta}_0) \xrightarrow{d} N\{\mathbf{0}, \mathbf{H}^{-1} \boldsymbol{\Sigma}(\boldsymbol{\delta}) \mathbf{H}^{-1}\}, \quad \text{as } n \rightarrow \infty.$$

where $\mathbf{H} = \lim_{n \rightarrow \infty} \mathbf{H}_n$ and $\boldsymbol{\Sigma}(\boldsymbol{\delta}) = \lim_{n \rightarrow \infty} \boldsymbol{\Sigma}_n(\boldsymbol{\delta})$.

Theorem 3.1 establishes the asymptotic normality of the parameter estimators. For the purpose of statistical inference, both $f_{ij}(\cdot)$ and $\boldsymbol{\delta}$ need to be estimated. To estimate density $f_{ij} \{Q_Y(\tau; \boldsymbol{\theta}_0 | \mathbf{W}_{ij})\}$ in \mathbf{H} , we adopt the quotient estimation method of Hendricks and Koenker (1992). The estimation of $\boldsymbol{\delta}$ in $\boldsymbol{\Sigma}(\boldsymbol{\delta})$ depends on the assumed correlation structure of \mathbf{Y}_i .

Next, we study theoretical properties of the GEE estimator. Let $\mathbf{G}_{il} = \mathcal{X}_i(\boldsymbol{\theta}_0)^T \mathbf{M}_{li} \boldsymbol{\Upsilon}_i \mathcal{X}_i(\boldsymbol{\theta}_0)$, where $\boldsymbol{\Upsilon}_i = \text{diag}(f_{ij} \{Q_Y(\tau; \boldsymbol{\theta}_0 | \mathbf{W}_{ij})\}, j = 1, \dots, n_i)$ and $\mathbf{G}_N = (\mathbf{G}_1^T, \dots, \mathbf{G}_v^T)^T$, where $\mathbf{G}_l = N^{-1} \sum_{i=1}^N \mathbf{G}_{il}$ for $l = 1, \dots, v$. Denote $\boldsymbol{\Xi}_{ll'}^0 = N^{-1} \sum_{i=1}^N \mathbf{S}_{il}(\boldsymbol{\theta}_0) \mathbf{S}_{il'}(\boldsymbol{\theta}_0)^T$ as the (l, l') th block of $\boldsymbol{\Xi}_N^0 = \{\boldsymbol{\Xi}_{ll'}^0\}_{l, l'=1}^v$. The following theorem establishes the asymptotic normality of the GEE estimator.

Theorem 3.2. *Suppose Assumptions (A1)-(A8) in the Web Appendix A hold, then under Model (2.2), there exists a local minimizer in (2.8) such that $\widehat{\boldsymbol{\theta}}^C$ is \sqrt{N} -consistent and*

asymptotically normal, that is

$$\sqrt{N}(\hat{\boldsymbol{\theta}}^C - \boldsymbol{\theta}_0) \xrightarrow{d} N\{\mathbf{0}, (\mathbf{G}^T \boldsymbol{\Xi}^{-1} \mathbf{G})^{-1}\}$$

where $\mathbf{G} = \lim_{N \rightarrow \infty} \mathbf{G}_N$ and $\boldsymbol{\Xi} = \lim_{N \rightarrow \infty} \boldsymbol{\Xi}_N^0$.

3.2 Selection consistency

Next, we establish the selection consistency of the Schwarz-type quantile information criterion to estimate the number of kink points.

Theorem 3.3. *Under the Assumptions (A1)-(A6) in the Web-Appendix A, we have that $P(\hat{K} = K_0) \rightarrow 1$ as $n \rightarrow \infty$.*

Theorem 3.3 demonstrates that the estimated \hat{K} via minimizing the SIC is equal to the true value K_0 with probability approaching 1 as the sample size n goes to infinity. In literature on change point detection such as Fryzlewicz et al. (2014) and Chan et al. (2014), the similar selection consistency for the number of change points has been also studied.

4 Testing the existence of kink points

In this section, we focus on testing whether there exists at least one kink point, without concerning the accurate number of kink points. To be specific, we are interested in the following null (H_0) and alternative (H_1) hypotheses,

$$H_0: \beta_k = 0, \text{ for all } k = 1, \dots, K. \text{ v.s. } H_1: \beta_k \neq 0 \text{ for some } k \in \{1, \dots, K\}. \quad (4.1)$$

To test (4.1), one may adopt the Wald-type test based on the asymptotic normality of the quantile estimator $\hat{\boldsymbol{\theta}}$. But it depends on the estimation of K . The use of likelihood ratio-based test is more complex as estimating K is also needed and the limiting distribution is much complicated. To avoid these problems, we turn to the score test based on the partial subgradient. Let $\boldsymbol{\xi} = (\alpha_0, \beta_0, \boldsymbol{\gamma}^T)^T$ and $\mathbf{U}_{ij} = (1, X_{ij}, \mathbf{Z}_{ij}^T)^T$. We define

$$R_n(t, \tau, \hat{\boldsymbol{\xi}}) = n^{-1/2} \sum_{i=1}^N \sum_{j=1}^{n_i} \psi_\tau(Y_{ij} - \hat{\boldsymbol{\xi}}^T \mathbf{U}_{ij})(X_{ij} - t)I(X_{ij} \leq t),$$

where $\hat{\boldsymbol{\xi}} = \arg \min \sum_{i,j} \rho_\tau(Y_{ij} - \boldsymbol{\xi}^T \mathbf{U}_{ij})$, which is the estimator without any kink point under the null hypothesis. $R_n(t, \tau, \hat{\boldsymbol{\xi}})$ can be regarded as the variant of the partial score of the quantile objective function with respect to β_1 at $\beta_1 = 0$ for the sub-sample with X_{ij} below t . The proposed score test statistic is

$$T_n(\tau) = \sup_{t \in \mathcal{T}} |R_n(t, \tau, \hat{\boldsymbol{\xi}})|, \quad (4.2)$$

where \mathcal{T} is the compact set for the kink point t . Intuitively, if the null hypothesis is true, the magnitudes of $R_n(t, \tau, \hat{\boldsymbol{\xi}})$ are relatively small which leads to the relative small value of $T_n(\tau)$; otherwise, the value of $T_n(\tau)$ is relatively large. The score test (4.2) can be regarded as a CUSUM-type test. This test statistic is computationally appealing since $R_n(t, \tau, \hat{\boldsymbol{\xi}})$ only requires estimating the model under the null hypothesis with no kink point so we avoid estimating either the number or the locations of kink points. As pointed by Qu (2008), the score-type test statistic is also applicable for multiple change/kink points situation.

To obtain the limiting distribution of $T_n(\tau)$, we introduce the following notations.

$$\hat{\mathbf{D}}_n = n^{-1} \sum_{i,j} \mathbf{U}_{ij} \mathbf{U}_{ij}^T \hat{f}_{ij}(\hat{\boldsymbol{\xi}}^T \mathbf{U}_{ij}), \quad \mathbf{D}_n = n^{-1} \sum_{i,j} \mathbf{U}_{ij} \mathbf{U}_{ij}^T f_{ij}(\boldsymbol{\xi}^T \mathbf{U}_{ij}).$$

We provide the following limiting distribution of $T_n(\tau)$ under H_0 .

Theorem 4.1. *Suppose that the Assumptions (A1)-(A6) and (A9) in the Web Appendix B hold. Under the null hypothesis H_0 , we have*

$$T_n(\tau) \Rightarrow \sup_{t \in \mathcal{T}} |R(t)|,$$

where $R(t)$ is a Gaussian process with mean zero and covariance function

$$\begin{aligned} \mathcal{W}(t, t') = n^{-1} & \left[\sum_{i=1}^N \sum_{j=1}^{n_i} \tau(1-\tau) \{ (X_{ij} - t)I(X_{ij} \leq t) - \mathbf{D}_1^T(t) \mathbf{D}^{-1} \mathbf{U}_{ij} \} \times \right. \\ & \left\{ (X_{ij} - t')I(X_{ij} \leq t') - \mathbf{D}_1^T(t') \mathbf{D}^{-1} \mathbf{U}_{ij} \right\} + \sum_{i=1}^N \sum_{j \neq j'} (\delta_{ijj'} - \tau^2) \{ (X_{ij} - t)I(X_{ij} \leq t) \\ & - \mathbf{D}_1^T(t) \mathbf{D}^{-1} \mathbf{U}_{ij} \} \left\{ (X_{ij'} - t')I(X_{ij'} \leq t') - \mathbf{D}_1^T(t') \mathbf{D}^{-1} \mathbf{U}_{ij'} \right\} \Big] \end{aligned}$$

where “ \Rightarrow ” denotes weak convergence, $\delta_{ijj'}$ is defined in Theorem 3.1 and $\mathbf{D}_1(t) = \lim_{n \rightarrow \infty} \mathbf{D}_{n1}(t)$ with $\mathbf{D}_{n1}(t) = n^{-1} \sum_{i,j} \mathbf{U}_{ij} (X_{ij} - t)I(X_{ij} \leq t) f_{ij}(\boldsymbol{\xi}^T \mathbf{U}_{ij})$.

Remark that the second part of the covariance function $\mathcal{W}(t, t')$ captures the within-subject correlations of the longitudinal data, which makes it different from the independent data.

Next, we derive the limiting distribution of the test statistic under the following local alternative model in Theorem 4.2,

$$Q_Y(\tau | \mathbf{W}_{ij}) = \alpha_0 + \beta_0 X_{ij} + n^{-1/2} \beta_1 (X_{ij} - t) I(X_{ij} \geq t) + \boldsymbol{\gamma}^T \mathbf{Z}_{ij}, \quad t \in \mathcal{T}. \quad (4.3)$$

Theorem 4.2. *Suppose that the assumptions in Theorem 4.1 hold. Under the local alternative model (4.3), we have*

$$T_n(\tau) \Rightarrow \sup_{t \in \mathcal{T}} |R(t) + q(t, \beta_1)|,$$

where $R(t)$ is the same as in Theorem 4.1, $q(t, \beta_1) = -\mathbf{D}_1^T(t) \mathbf{D}^{-1} \mathbf{D}_2(t, \beta_1)$ and $\mathbf{D}_2(t, \beta_1) = \lim_{n \rightarrow \infty} \mathbf{D}_{n2}(t, \beta_1)$ with $\mathbf{D}_{n2}(t, \beta_1) = n^{-1} \sum_{i,j} \mathbf{U}_{ij} \beta_1 (X_{ij} - t) I(X_{ij} > t) f_{ij}(\boldsymbol{\xi}^T \mathbf{U}_{ij})$.

However, the limiting null distribution of $T_n(\tau)$ takes the non-standard form and its critical values as well as the P-values can not be tabulated directly. To calculate the P-values numerically, we first define an asymptotic representation of $R_n(t)$ as

$$R_n^*(t) = n^{-1/2} \sum_{i=1}^N \vartheta_i \sum_{j=1}^{n_i} \psi_\tau(Y_{ij} - \mathbf{U}_{ij}^T \hat{\boldsymbol{\xi}}) \left\{ (X_{ij} - t) I(X_{ij} \leq t) - \hat{\mathbf{D}}_{n1}(t) \hat{\mathbf{D}}_n^{-1} \mathbf{U}_{ij} \right\},$$

where $\hat{\mathbf{D}}_{n1}(t) = n^{-1} \sum_{i,j} \mathbf{U}_{ij} (X_{ij} - t) I(X_{ij} \leq t) \hat{f}_{ij}(\hat{\boldsymbol{\xi}}^T \mathbf{U}_{ij})$ and $\{\vartheta_i; i = 1, \dots, N\}$ are a random sample from the standard normal distribution. Theorem 4.3 shows the asymptotic representation $R_n^*(t)$ shares the same limiting null distribution of $R_n(t)$.

Theorem 4.3. *Suppose that the assumptions in Theorem 4.1 hold, under the null hypothesis, $R_n^*(t)$ converges to the Gaussian process $R(t)$ defined in Theorem 4.1 as $n \rightarrow \infty$.*

Then, we develop a modified blockwise wild bootstrap method in Algorithm 1 based on $R_n^*(t)$ to characterize the limiting null distribution of $T_n(\tau)$.

Algorithm 1 A modified blockwise wild bootstrap method

Step 1. Calculate the test statistic $T_n(\tau)$ using the original data.

Step 2. Generate $\{\vartheta_i; i = 1, \dots, N\}$ from the standard normal distribution and calculate the bootstrapped test statistic $T_n^*(\tau) = \sup_{t \in \mathcal{T}} |R_n^*(t)|$.

Step 3. Repeat Steps 1-2 B times to get $\{T_{nb}^*(\tau), b = 1, \dots, B\}$. The empirical P-value is the proportion of $T_{nb}^*(\tau)$'s exceeding $T_n(\tau)$ i.e. $\hat{p}_n = B^{-1} \sum_{b=1}^B I\{T_{nb}^*(\tau) \geq T_n(\tau)\}$.

5 Simulation Studies

5.1 Model descriptions

In this section, two data generation processes (DGPs) are considered to evaluate the finite sample performance of the proposed methods, including the asymptotic performance of two kinds of parameter estimators and the performance of the proposed score test procedure.

DGP 1: We generate data from the following model,

$$Y_{ij} = \alpha_0 + \alpha_1 X_{ij} + \gamma Z_{ij} + \sum_{k=1}^K \beta_k (X_{ij} - t_k) I(X_{ij} > t_k) + e_{ij}, \quad (5.1)$$

where $i = 1, \dots, N, j = 1, \dots, n_i$, $(\alpha_0, \alpha_1, \gamma) = (1, 1, 0.2)$ are fixed and e_{ij} 's are the error terms. Similar to Li et al. (2015), we consider three different cases: Case 1 (Compound Symmetry Correlation Structure), $e_{ij} = a_i + \epsilon_{ij}$, where $a_i \stackrel{i.i.d}{\sim} N(0, 1)$ and $\epsilon_{ij} \stackrel{i.i.d}{\sim} t_3$; Case 2 (AR(1) Correlation Structure), $e_{ij} = v(X_{ij})u_{ij}$ where $v(x) = 3.2 - 0.2x$, $u_{ij} = 0.5u_{i,j-1} + \epsilon_{ij}$ and $\epsilon_{ij} \stackrel{i.i.d}{\sim} N(0, 1)$ and Case 3 (Heteroscedastic Correlation Structure), $e_{ij} = a_i + g(X_{ij})\epsilon_{ij}$ where $g(x) = \sqrt{(3.2 - 0.2x)^2 - 1}$, $a_i \stackrel{i.i.d}{\sim} N(0, 1)$ and $\epsilon_{ij} \stackrel{i.i.d}{\sim} N(0, 1)$. In the Cases 1 and 3, $X_{ij} \stackrel{i.i.d}{\sim} U(0, 10)$ and $Z_{ij} \stackrel{i.i.d}{\sim} U(0, 10)$. In Case 2, $X_{i1} \stackrel{i.i.d}{\sim} U(0.5, 7.5)$, $X_{ij} = X_{i,j-1} + 0.5$ for $j > 1$, and $Z_{ij} \stackrel{i.i.d}{\sim} U(0, 10)$. For each case, we let $n_i \in \{6, 7, 8, 9, 10\}$ with equal size $N/5$ for each element to add imbalance to the number of observations per subject. The size of total observations is $n = 8N$. For all cases, the simulation was repeated 1000 times with the number of subjects $N = 100, 200, 400, 800$ and 1600, respectively.

DGP 2: To evaluate the applicability of the proposed methods for the progesterone data analysis, we consider the similar model structure as in DGP 1 expect that X_{ij} is the day in cycles and Z_{ij} is an indicator taking 1 for the conceptive woman and 0 for non-conceptive woman in the progesterone data, see more details in Section 6. Let $(\alpha_0, \alpha_1, \gamma) = (-1, 0, 0.5)$ and the error term settings are the same as in DGP 1.

5.2 Selection consistency and parameter estimation

We first check the selection consistency of \hat{K} in Theorem 3.3. Three different kink effects are considered. For DGP 1, we set (1) $K = 1$ with $\beta_1 = -2$ and $t_1 = 5$; (2) $K = 2$ with $(\beta_1, \beta_2) = (-2, 2)$ and $(t_1, t_2) = (3, 6)$; (3) $K = 3$ with $(\beta_1, \beta_2, \beta_3) = (-2, 2, -2)$ and $(t_1, t_2, t_3) = (3, 5, 8)$. For DGP 2, we set (1) $K = 1$ with $\beta_1 = 0.5$ and $t_1 = 1$; (2) $K = 2$ with $(\beta_1, \beta_2) = (0.5, -0.5)$ and $(t_1, t_2) = (-1, 6)$; (3) $K = 3$ with $(\beta_1, \beta_2, \beta_3) = (0.5, -0.5, 0.5)$

and $(t_1, t_2, t_3) = (-2, 4, 10)$. We consider quantile levels 0.25, 0.5 and 0.75, and repeat the simulation for each case 1000 times. Table 1 reports the percentages of the estimated \hat{K} 's equaling to the true K_0 and the average running time across 1000 repetitions for DGPs 1-2. We denote "WI" and "WC" as the estimator under the working independence framework and the GEE estimator via incorporating the working correlation structures, respectively.

We observe that as the number of individuals N increases, the selection rates gradually approach to 100% for all cases across different K 's, which illustrates the selection consistency in Theorem 3.3. For DGP 1, it is obvious that the GEE estimator via incorporating the correlation information can effectively improve the selection rates across all cases with the price of much more computing time, and such phenomenon is even pronounced for $K = 3$. However, for DGP 2, incorporating the correlation seems not to improve the selection rates. The possible reason is that the within-subject correlations may be weak in the progesterone data and the estimator under the working independence framework can still perform satisfactorily.

Next, we evaluate the finite sample performance of two proposed methods as well as the least squared (LS) estimator. For saving space, we only report the parameter estimation results of $K = 2$ for DGP 1 when $N = 400$ and DGP 2 for all error cases in Table 2. The remaining results for DGP 1 based on $N = 200, 800$ and 1600 for each case are given in the Web Appendix C in the supplement. As shown in the Table, all the parameter estimates have sufficiently small biases and the biases diminish to zero as the sample size increases, which demonstrates the consistency of the estimators. Besides, the Monte Carlo standard deviations (SD) are quite close to the estimated standard error (ESE) especially as N increases, which validates that the derived limiting distribution provides reasonable asymptotic variances. The coverage rates of 95% Wald confidence intervals (CovP) for the regression coefficients $(\alpha_0, \alpha_1, \gamma, \beta_1, \beta_2)$ are very close to the nominal level 95%, while those for kink points (t_1, t_2) are relatively indecent. But when the number of individuals increases to $N = 1600$, their CovPs also becomes the nominal level. More discussions on the CovPs for kink points are included in the Appendix C. In summary, the methods based on quantile regression can generally perform better than the least squared estimators especially for heteroscedastic errors. The GEE estimators via incorporating the working correlations within subjects are generally more efficient than the estimators under the working independence framework.

We remark that the asymptotic variances of the WI estimators under the working independence framework are based on the correlation structure parameter δ . Following Li et al. (2015), we adopt a general form to obtain the covariance matrix estimation for $\Sigma(\delta)$ in Theorem 3.1. To be specific, $\delta_{ijj'} - \tau^2$ here can be estimated by $I(\hat{e}_{ij} < 0, \hat{e}_{ij'} <$

Table 1: The percentages of correctly selecting $\hat{K} = K$ ($K = 1, 2, 3$) as well as their average running time (in second) of two different estimation strategies for DGPs 1-2. The results of DGP 1 are obtained across sample sizes $N = 200, 400, 800$ and 1600.

K	N		Correctly Selected Rate						Average Running Time (in second)					
			WI			WC			WI			WC		
			0.25	0.5	0.75	0.25	0.5	0.75	0.25	0.5	0.75	0.25	0.5	0.75
DGP 1														
1	100	Case 1	0.978	0.992	0.982	0.992	0.994	0.988	1.134	1.168	1.270	3.719	3.428	3.859
		Case 2	0.976	0.988	0.962	0.996	0.996	0.988	1.093	1.108	1.282	3.812	3.586	4.059
		Case 3	0.976	0.988	0.972	0.990	0.994	0.994	1.117	1.142	1.255	3.648	3.395	3.735
	200	Case 1	0.976	0.994	0.990	0.992	1.000	0.994	1.822	1.999	2.174	6.460	6.025	6.915
		Case 2	0.974	0.992	0.984	0.990	0.994	0.998	1.741	1.899	2.045	6.561	6.340	7.062
		Case 3	0.970	0.988	0.968	0.982	0.996	0.984	1.786	1.959	2.179	6.250	5.947	6.801
	400	Case 1	0.996	0.994	0.998	0.998	0.998	1.000	3.304	4.085	4.579	11.198	10.891	12.483
		Case 2	0.986	0.990	0.970	0.994	0.996	0.988	3.171	3.818	4.444	10.915	11.022	12.471
		Case 3	0.990	0.994	0.990	0.994	1.000	0.994	3.335	3.919	4.672	10.484	10.186	11.991
	800	Case 1	0.990	1.000	0.986	0.996	1.000	0.998	8.136	10.861	12.945	22.083	22.716	26.511
		Case 2	0.990	0.998	0.982	0.996	1.000	0.990	7.378	9.776	11.673	21.739	22.741	26.576
		Case 3	0.984	0.998	0.996	0.990	1.000	1.000	8.109	10.330	12.155	20.776	21.949	25.310
	1600	Case 1	0.992	0.990	0.990	0.996	0.992	0.994	22.635	32.013	37.940	47.065	53.765	62.473
		Case 2	0.990	0.992	0.986	0.996	0.992	0.988	18.679	26.835	33.049	43.580	50.221	59.142
		Case 3	0.982	0.992	0.988	0.988	0.992	0.990	17.546	24.537	29.091	34.695	39.894	46.472
2	100	Case 1	0.964	0.976	0.968	0.986	0.980	0.980	1.981	2.009	2.153	4.033	3.848	4.223
		Case 2	0.944	0.962	0.952	0.948	0.972	0.958	1.878	1.939	1.960	4.114	3.970	4.129
		Case 3	0.966	0.986	0.982	0.980	0.988	0.988	1.968	1.918	2.102	3.973	3.757	4.114
	200	Case 1	0.966	0.976	0.960	0.988	0.980	0.980	3.288	3.561	3.983	7.178	7.042	7.834
		Case 2	0.980	0.986	0.990	0.986	0.990	0.994	3.029	3.314	3.654	7.336	7.174	7.954
		Case 3	0.972	0.972	0.978	0.972	0.973	0.982	3.218	3.609	3.840	7.171	7.064	7.706
	400	Case 1	0.978	0.978	0.966	0.982	0.980	0.970	6.340	7.693	8.668	13.559	14.111	15.959
		Case 2	0.986	0.982	0.978	0.988	0.986	0.980	5.478	6.538	7.678	13.225	13.439	15.406
		Case 3	0.970	0.978	0.968	0.972	0.984	0.974	5.871	6.804	7.936	12.662	12.697	14.679
	800	Case 1	0.970	0.972	0.978	0.976	0.974	0.978	14.112	19.039	22.015	26.742	30.280	34.640
		Case 2	0.966	0.990	0.970	0.968	0.992	0.976	12.719	16.223	20.050	27.079	29.265	34.196
		Case 3	0.986	0.974	0.970	0.992	0.978	0.976	13.529	18.367	21.998	26.285	29.776	34.702
	1600	Case 1	0.986	0.988	0.966	0.986	0.988	0.968	37.306	54.870	65.828	60.859	75.764	88.928
		Case 2	0.972	0.990	0.974	0.972	0.990	0.980	29.898	43.507	54.844	55.356	66.385	79.601
		Case 3	0.970	0.984	0.972	0.970	0.984	0.972	33.575	49.053	60.632	55.736	69.157	82.570
3	100	Case 1	0.892	0.914	0.879	0.898	0.926	0.897	3.033	3.142	3.467	4.316	4.374	4.816
		Case 2	0.834	0.908	0.866	0.886	0.911	0.884	2.881	3.183	3.131	4.268	4.543	4.578
		Case 3	0.875	0.916	0.887	0.852	0.926	0.892	3.142	3.118	3.407	4.377	4.330	4.601
	200	Case 1	0.922	0.934	0.920	0.937	0.940	0.922	4.834	5.873	6.287	7.189	7.988	8.607
		Case 2	0.916	0.926	0.915	0.921	0.932	0.916	4.583	5.030	6.014	7.170	7.457	8.480
		Case 3	0.937	0.948	0.928	0.941	0.951	0.931	4.911	5.151	6.138	7.125	7.242	8.439
	400	Case 1	0.955	0.964	0.956	0.958	0.968	0.962	9.610	11.827	13.326	13.638	15.656	17.508
		Case 2	0.929	0.955	0.948	0.931	0.959	0.933	8.558	10.751	11.617	12.996	15.174	15.894
		Case 3	0.932	0.957	0.951	0.935	0.964	0.957	8.854	11.039	12.605	12.769	14.830	16.607
	800	Case 1	0.958	0.976	0.976	0.960	0.983	0.978	20.928	28.144	33.776	28.268	34.774	41.035
		Case 2	0.946	0.971	0.958	0.952	0.975	0.964	17.059	24.043	30.399	24.611	31.537	38.972
		Case 3	0.964	0.984	0.967	0.970	0.988	0.973	18.152	26.441	31.027	25.054	33.069	38.561
	1600	Case 1	0.986	0.984	0.988	0.986	0.984	0.990	58.955	86.495	93.822	72.267	99.062	99.383
		Case 2	0.975	0.979	0.964	0.976	0.979	0.968	47.195	70.414	93.301	61.775	84.341	98.438
		Case 3	0.973	0.975	0.968	0.973	0.975	0.968	49.381	78.154	95.104	61.952	90.252	97.583
DGP 2														
1		Case 1	0.996	1.000	0.996	0.990	0.999	0.970	1.260	1.239	1.304	3.118	2.658	3.202
		Case 2	0.956	0.983	0.944	0.956	0.982	0.928	1.448	1.350	1.513	3.631	3.100	3.768
		Case 3	0.996	0.998	0.994	0.955	0.998	0.970	1.281	1.239	1.335	3.184	2.668	3.248
2		Case 1	0.998	1.000	0.998	0.977	0.996	0.956	2.854	2.769	2.769	5.441	4.705	5.414
		Case 2	0.988	0.992	0.984	0.924	0.994	0.901	3.060	3.004	2.989	6.333	5.309	6.415
		Case 3	0.998	0.999	1.000	0.960	0.999	0.958	2.912	2.819	2.866	5.613	4.759	5.576
3		Case 1	0.981	0.986	0.968	0.647	0.969	0.476	6.581	6.231	6.465	8.439	9.038	7.238

Table 2: Simulation results of two proposed methods (WI and WC) and the LS method across 1000 repetitions for DGP 1 with $N = 400$ and DGP 2 when $K = 2$.

	WI					WC					LS				
	Bias	SD	ESE	MSE	CovP	Bias	SD	ESE	MSE	CovP	Bias	SD	ESE	MSE	CovP
DGP 1, Case 1															
α_0	0.010	0.184	0.183	0.034	0.956	0.005	0.147	0.152	0.021	0.944	0.009	0.172	0.173	0.029	0.956
α_1	0.001	0.014	0.014	0.000	0.960	0.001	0.011	0.012	0.000	0.970	0.000	0.014	0.014	0.000	0.950
β_1	-0.004	0.094	0.089	0.009	0.924	-0.002	0.070	0.070	0.005	0.948	-0.003	0.082	0.083	0.007	0.942
β_2	-0.009	0.132	0.127	0.018	0.942	-0.003	0.098	0.100	0.010	0.946	-0.013	0.125	0.118	0.016	0.930
γ	0.020	0.111	0.107	0.013	0.954	0.007	0.085	0.085	0.007	0.948	0.020	0.103	0.100	0.011	0.938
t_1	0.012	0.127	0.109	0.016	0.908	0.005	0.094	0.087	0.009	0.926	0.013	0.110	0.101	0.012	0.910
t_2	0.000	0.121	0.101	0.015	0.898	-0.001	0.090	0.081	0.008	0.918	-0.008	0.117	0.094	0.014	0.896
DGP 1, Case 2															
α_0	0.009	0.346	0.356	0.119	0.950	0.008	0.296	0.284	0.087	0.924	0.002	0.294	0.300	0.087	0.960
α_1	0.000	0.020	0.020	0.000	0.948	0.000	0.016	0.016	0.000	0.946	0.000	0.018	0.018	0.000	0.952
β_1	0.007	0.194	0.177	0.038	0.930	0.001	0.152	0.136	0.023	0.908	0.008	0.154	0.143	0.024	0.936
β_2	-0.042	0.224	0.230	0.052	0.962	-0.026	0.178	0.178	0.032	0.950	-0.033	0.179	0.184	0.033	0.958
γ	0.040	0.167	0.157	0.029	0.940	0.027	0.124	0.123	0.016	0.952	0.030	0.132	0.127	0.018	0.946
t_1	0.018	0.236	0.192	0.056	0.876	0.015	0.175	0.151	0.031	0.898	0.007	0.187	0.155	0.035	0.882
t_2	-0.013	0.158	0.138	0.025	0.910	-0.016	0.117	0.108	0.014	0.904	-0.011	0.126	0.112	0.016	0.908
DGP 1, Case 3															
α_0	-0.023	0.287	0.281	0.083	0.936	-0.009	0.241	0.230	0.058	0.948	-0.021	0.266	0.258	0.071	0.936
α_1	0.000	0.018	0.018	0.000	0.956	-0.001	0.015	0.015	0.000	0.960	0.001	0.015	0.016	0.000	0.964
β_1	0.010	0.152	0.143	0.023	0.938	0.007	0.124	0.114	0.015	0.932	0.007	0.140	0.131	0.019	0.924
β_2	-0.030	0.190	0.189	0.037	0.956	-0.015	0.150	0.149	0.023	0.946	-0.019	0.168	0.170	0.028	0.942
γ	0.021	0.146	0.133	0.022	0.932	0.008	0.112	0.105	0.012	0.940	0.011	0.122	0.116	0.015	0.942
t_1	0.015	0.190	0.160	0.036	0.922	0.004	0.150	0.127	0.023	0.906	0.009	0.168	0.144	0.028	0.914
t_2	-0.001	0.140	0.120	0.020	0.892	0.001	0.104	0.096	0.011	0.938	-0.003	0.116	0.103	0.013	0.896
DGP 2, Case 1															
α_0	-0.034	0.217	0.204	0.048	0.926	-0.023	0.202	0.193	0.044	0.906	-0.023	0.212	0.199	0.046	0.936
α_1	0.001	0.282	0.236	0.079	0.901	0.007	0.263	0.262	0.069	0.952	0.006	0.263	0.256	0.069	0.938
β_1	-0.005	0.032	0.031	0.001	0.932	-0.004	0.028	0.028	0.001	0.928	-0.003	0.032	0.030	0.001	0.946
β_2	0.010	0.048	0.048	0.002	0.934	0.009	0.042	0.043	0.002	0.950	0.011	0.050	0.048	0.003	0.940
γ	-0.009	0.046	0.045	0.002	0.944	-0.007	0.039	0.040	0.002	0.952	-0.011	0.048	0.045	0.002	0.934
t_1	-0.007	0.406	0.385	0.164	0.940	0.006	0.365	0.349	0.133	0.924	0.032	0.412	0.377	0.170	0.942
t_2	0.008	0.392	0.376	0.153	0.938	0.002	0.341	0.342	0.116	0.940	-0.016	0.384	0.373	0.147	0.948
DGP 2, Case 2															
α_0	-0.027	0.228	0.222	0.053	0.938	-0.021	0.219	0.192	0.049	0.922	-0.036	0.253	0.251	0.065	0.944
α_1	-0.004	0.164	0.156	0.027	0.936	-0.006	0.166	0.141	0.028	0.910	-0.005	0.193	0.189	0.037	0.940
β_1	-0.004	0.039	0.039	0.002	0.938	-0.003	0.037	0.032	0.001	0.928	-0.006	0.046	0.045	0.002	0.934
β_2	0.018	0.066	0.065	0.005	0.936	0.012	0.063	0.057	0.004	0.916	0.025	0.082	0.076	0.007	0.928
γ	-0.019	0.065	0.063	0.005	0.930	-0.013	0.063	0.056	0.004	0.912	-0.026	0.077	0.073	0.007	0.940
t_1	0.048	0.527	0.462	0.280	0.914	0.026	0.486	0.385	0.236	0.901	0.063	0.546	0.497	0.302	0.914
t_2	-0.012	0.485	0.455	0.235	0.920	0.009	0.460	0.383	0.211	0.910	-0.033	0.656	0.503	0.430	0.876
DGP 2, Case 3															
α_0	-0.036	0.220	0.205	0.050	0.922	-0.029	0.211	0.185	0.046	0.908	-0.040	0.232	0.209	0.055	0.928
α_1	0.034	0.270	0.265	0.074	0.940	0.029	0.273	0.236	0.075	0.916	0.024	0.266	0.262	0.071	0.936
β_1	-0.003	0.032	0.032	0.001	0.936	-0.003	0.029	0.029	0.001	0.942	-0.005	0.035	0.033	0.001	0.938
β_2	0.015	0.053	0.050	0.003	0.952	0.011	0.047	0.045	0.002	0.958	0.016	0.052	0.050	0.003	0.950
γ	-0.015	0.048	0.047	0.003	0.944	-0.011	0.042	0.042	0.002	0.948	-0.016	0.052	0.047	0.003	0.920
t_1	0.038	0.405	0.395	0.165	0.938	0.027	0.376	0.361	0.142	0.932	0.025	0.464	0.402	0.215	0.908
t_2	-0.028	0.409	0.386	0.168	0.932	-0.028	0.365	0.353	0.134	0.948	-0.025	0.437	0.388	0.192	0.940

Note: Bias is empirical bias; SD is the Monte Carlo standard deviation; ESE is the estimated standard error; MSE is the mean square error and CovP is the coverage probability of 95% Wald confidence interval.

$0) - 2^{-1}\tau \{I(\hat{e}_{ij} < 0) + I(\hat{e}_{ij'} < 0)\}$, where \hat{e}_{ij} 's are estimated residuals. In real data analysis, we also adopt this general form to approximately depict the within-subject correlations. For the GEE estimator using the QIF approach, we choose three basis matrices \mathbf{M}_{1i} , \mathbf{M}_{2i} and \mathbf{M}_{3i} as specified in Section 2.2.2 to incorporate within-subject correlation.

5.3 Power analysis

Next, we evaluate the performance of the proposed testing procedure for the existence of the kink points using simulations. We consider varying kink effects with $K = 1$ and 2 kink points and other parameters remain unchanged as DGPs 1-2. For DGP 1, we let $\beta_1 = 0, 0.1, 0.3, 0.5, 0.7$ for $K = 1$ and $\beta_1 = -\beta_2 = 0, 0.1, 0.3, 0.5, 0.7$ for $K = 2$, and for DGP 2, $\beta_1 = 0, 0.03, 0.05, 0.08, 0.1$ for $K = 1$ and $\beta_1 = -\beta_2 = 0, 0.1, 0.2, 0.3, 0.4$ for $K = 2$. For each scenario, we conduct 10000 repetitions for the type I error i.e. when there is no kink point and 1000 repetitions for the power when kink points exist. The P-values of the quantile score test are computed by using 300 bootstrap replicates i.e. $B = 300$ in Algorithm 1.

The results including the average running time are summarized in Tables 8-9 in the Appendix D of the supplement. Figure 1 depicts the empirical power curves across $\tau = 0.1, 0.25, 0.5, 0.75$ and 0.9 for Cases 1-3 with $K = 1$ kink point and the results for $K = 2$ is showed in the Web Appendix D. As shown in the Figure, when $\beta_1 = 0$, i.e. under the null hypothesis, the type I errors are reasonably close to the nominal level 5%, which suggests that our proposed quantile score test can control the type I errors. As β_1 increases, i.e. the kink effect gets enhanced, the local powers gradually approach to one for all quantiles. We also observe that the powers at the tail quantile levels (e.g. $\tau = 0.1$ and 0.9) approach at a slower rate than that at the moderate quantile levels such as $\tau = 0.5$. It is common due to the asymmetry of observations at extreme quantiles and can be alleviated by increasing the sample size. Therefore, we conclude that the score-based test can also identify the existence of kink points well.

6 Progesterone Data Analysis

In this section, we analyze the longitudinal progesterone data in Munro et al. (1991). This longitudinal research followed a total of 51 women with healthy reproductive function enrolled in an artificial insemination clinic. The data set consists of two groups: conceptive and non-conceptive. In the non-conceptive group, the urinary metabolite progesterone was mea-

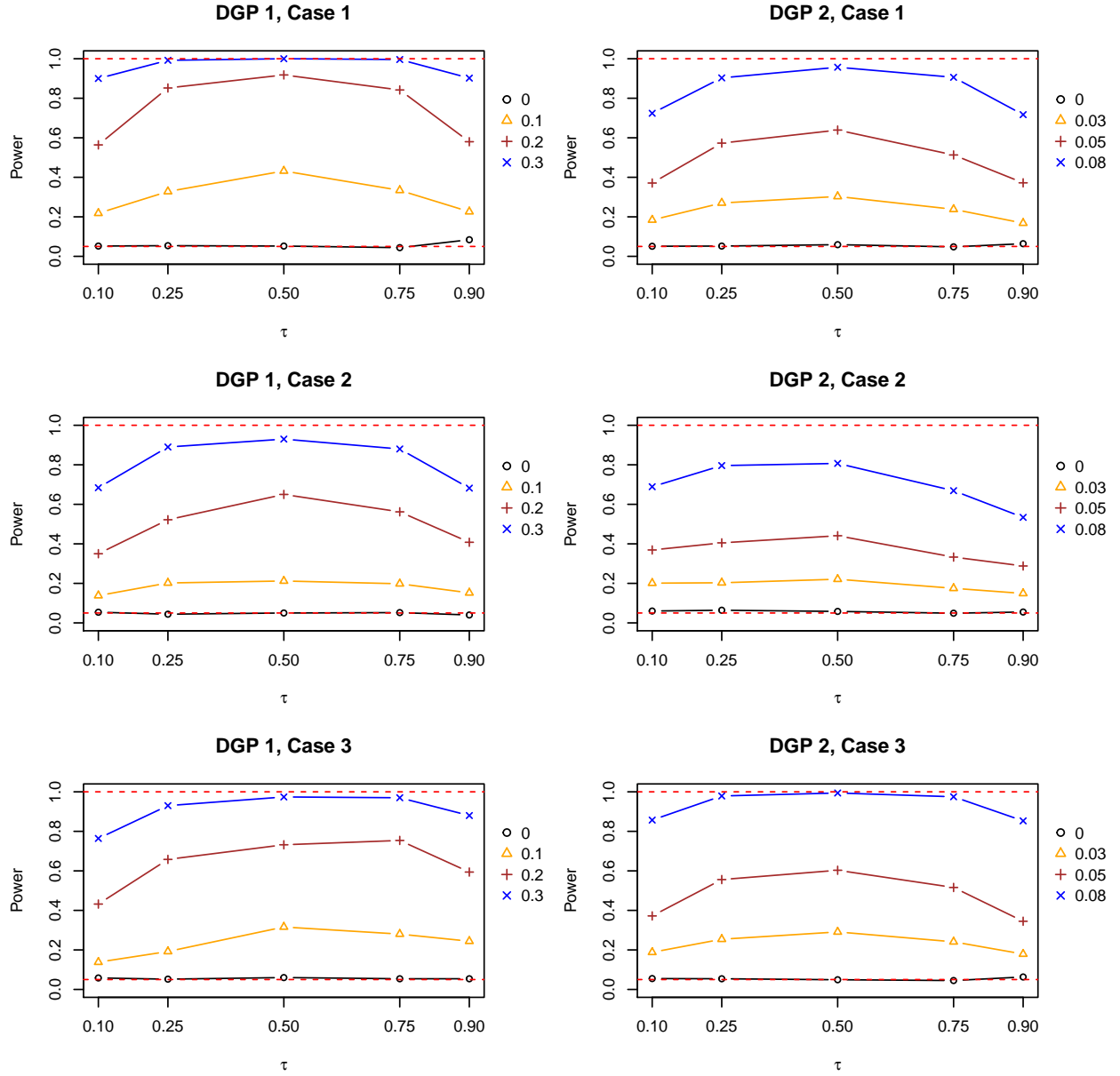


Figure 1: The local empirical powers when $K = 1$ for DGP 1 with $N = 400$ and DGP 2 across $\tau = 0.10, 0.25, 0.50, 0.75, 0.90$. We conduct 10000 repetitions for the Type I errors and 1000 repetitions for the local powers. The bottom and upside red dashed lines represent the nominal level 0.05 and 1, respectively.

sured for one to five menstrual cycles for a woman while in the conceptive group, each woman only contributed for one menstrual cycle. There are 22 conceptive and 69 non-conceptive women' menstrual cycles. At each cycle, the measurements were recorded per day from 8 days before the day of ovulation and until 15 days after the ovulation, totally 24 days in a cycle. To make the progesterone curves have the same design point, the data had been

aligned and truncated by the day of ovulation (Day 0). However, due to some reason, not all measurements in a cycle are fully observed, which results in some missing values. After removing these values, we get a sample size of 2004 observations among $N = 91$ women's menstrual cycles with each cycles contributing from 9 to 24 observations.

Several researchers includes Brumback and Rice (1998), Fan and Zhang (2000) and Wu and Zhang (2002) have analyzed this data set by using nonparametric regression methods. All these researches suggested that there exists nonlinear effect between the logarithmic progesterone and the day in cycles. Figure 2 presents a plot for the 91 progesterone curves. The logarithmic progesterone remains rather stable at first 8 days, but rises sharply after ovulation. The uptrend persists several days and then drops slightly. It seems that the progesterone curves experience two structural changes but the number remains to be identified. To validate this observation and identify the locations of kink points, we re-analyze the data using the proposed MKQR model for the longitudinal data,

$$Y_{ij} = \alpha_0 + \alpha_1 X_{ij} + \sum_{k=1}^K \beta_k (X_{ij} - t_k)_+ + \gamma Z_{ij} + e_{ij}, \quad (6.1)$$

where Y_{ij} is the j th observed log-progesterone of the i th cycle, X_{ij} is the day in cycles and Z_{ij} is an indicator taking 1 for the conceptive woman and 0 for non-conceptive woman. $\boldsymbol{\eta} = (\alpha_0, \alpha_1, \beta_1, \dots, \beta_K, \gamma)^T$ are the unknown coefficients and (t_1, \dots, t_K) are the unknown locations of kink points. We consider different quantiles $\tau = 0.1, 0.25, 0.5, 0.75$ and 0.9 .

We first check the existence of kink points by using the proposed test with 500 bootstrap replicates for all quantiles. The resulting P-values are all nearly 0, suggesting a highly significant kink change for the slope of the day in cycle. We then select the number of kink points by using the Schwarz-type information criterion and identify two kink points for both methods. Table 3 summarizes the parameter estimation results of two proposed estimation methods at different quantiles. In general, the working independence (WI) estimators are quite close to the GEE estimators with incorporating the working within-subject correlations (WC). In most cases, the WC estimators can achieve smaller standard errors than the WI estimators, which shows that the efficiency gain can be obtained by considering the within-subject correlations in the longitudinal data analysis.

Based on the estimation results, we obtain the following main findings. It is obvious that two kink points are detected for all quantiles and divide the day in the menstrual cycle into three stages. At the first stage, the log-progesterone values stay almost unchanged with the increase of the day, as the estimated $\hat{\alpha}_1$'s are close to 0 for all quantiles. In the second stage, the log-progesterone experiences a significant rise ($\hat{\beta}_1 + \hat{\alpha}_1 > 0$ for all quantiles) after the first

estimated kink point around -0.3 to -1.3. At the location around 4.5 to 5.5, the relationship between the log-progesterone and the day in cycle experiences a new structural change once again. After the second kink points, it seems that the progesterone values for the women decrease at lower quantiles $\tau = 0.1, 0.25$ while it goes back to be stable for upper quantiles ($\tau = 0.75, 0.9$). Figure 2 highlights the above finding through the fitted quantile curves. In conclusion, the progesterone level remains stable before the day of ovulation, then increases quickly in five to six days after ovulation and then changes to stable again or even drops slightly after the second kink point.

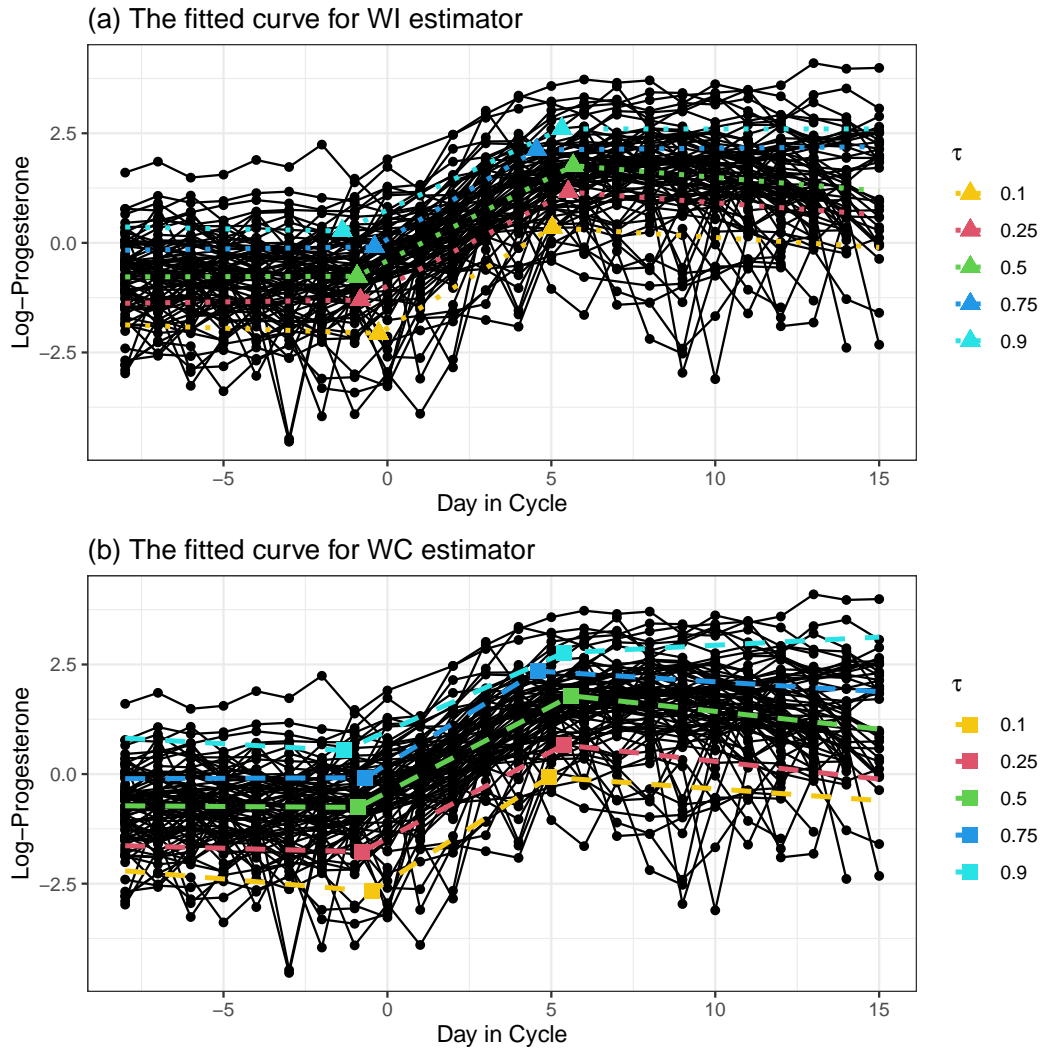


Figure 2: Scatter plots between the logarithm of progesterone and the day in cycle with the fitted curves for (a) the estimator under the working independence framework (WI) and (b) the GEE estimator incorporating the working correlations (WC) at quantile levels 0.1, 0.25, 0.5, 0.75 and 0.9. \blacktriangle and \blacksquare denotes the estimated kink points using different methods.

Table 3: The estimated parameters and their standard errors (in parentheses) for the progesterone data. P-values are computed by using the proposed score test based on 500 bootstrap replicates. C.I. denotes the 95% Wald-type confidence interval.

Method	τ	0.1	0.25	0.5	0.75	0.9
	P-values	0.005	0.000	0.000	0.000	0.000
WI	\widehat{K}	2	2	2	2	2
	$\widehat{\alpha}_0$	-2.071 _(0.221)	-1.297 _(0.136)	-0.760 _(0.110)	-0.212 _(0.110)	0.234 _(0.118)
	C.I.	[-2.505, -1.637]	[-1.565, -1.030]	[-0.977, -0.544]	[-0.427, 0.004]	[0.003, 0.465]
	$\widehat{\alpha}_1$	-0.025 _(0.028)	0.010 _(0.014)	0.002 _(0.011)	0.010 _(0.087)	-0.014 _(0.031)
	C.I.	[-0.080, 0.031]	[-0.019, 0.039]	[-0.019, 0.023]	[-0.024, 0.044]	[-0.074, 0.047]
	$\widehat{\beta}_1$	0.480 _(0.092)	0.379 _(0.024)	0.381 _(0.018)	0.438 _(0.041)	0.362 _(0.031)
	C.I.	[0.300, 0.661]	[0.333, 0.426]	[0.345, 0.417]	[0.357, 0.518]	[0.296, 0.427]
	$\widehat{\beta}_2$	-0.500 _(0.108)	-0.444 _(0.028)	-0.445 _(0.026)	-0.441 _(0.037)	-0.348 _(0.038)
	C.I.	[-0.712, -0.288]	[-0.499, -0.390]	[-0.495, -0.395]	[-0.513, -0.369]	[-0.422, -0.274]
	$\widehat{\gamma}$	0.331 _(0.377)	0.256 _(0.163)	0.205 _(0.146)	0.124 _(0.177)	0.016 _(0.359)
	C.I.	[-0.407, 1.069]	[-0.064, 0.575]	[-0.082, 0.491]	[-0.223, 0.471]	[-0.687, 0.719]
	\widehat{t}_1	-0.271 _(0.541)	-0.824 _(0.203)	-0.925 _(0.211)	-0.390 _(0.329)	-1.376 _(0.390)
	C.I.	[-1.331, 0.790]	[-1.222, -0.426]	[-1.339, -0.510]	[-1.036, 0.255]	[-2.141, -0.612]
	\widehat{t}_2	5.029 _(0.420)	5.516 _(0.312)	5.666 _(0.148)	4.548 _(0.223)	5.319 _(0.686)
	C.I.	[4.205, 5.853]	[4.904, 6.127]	[5.377, 5.956]	[4.110, 4.986]	[3.975, 6.662]
WC	\widehat{K}	2	2	2	2	2
	$\widehat{\alpha}_0$	-2.703 _(0.195)	-1.786 _(0.130)	-0.764 _(0.073)	-0.081 _(0.114)	0.817 _(0.157)
	C.I.	[-3.086, -2.321]	[-2.042, -1.531]	[-0.908, -0.620]	[-0.304, 0.142]	[0.510, 1.124]
	$\widehat{\alpha}_1$	-0.062 _(0.028)	-0.019 _(0.016)	-0.005 _(0.008)	0.003 _(0.016)	-0.042 _(0.023)
	C.I.	[-0.117, -0.007]	[-0.050, 0.012]	[-0.020, 0.010]	[-0.027, 0.034]	[-0.087, 0.002]
	$\widehat{\beta}_1$	0.544 _(0.096)	0.415 _(0.038)	0.397 _(0.012)	0.460 _(0.038)	0.374 _(0.025)
	C.I.	[0.356, 0.733]	[0.341, 0.490]	[0.373, 0.422]	[0.385, 0.535]	[0.325, 0.424]
	$\widehat{\beta}_2$	-0.535 _(0.089)	-0.477 _(0.043)	-0.473 _(0.019)	-0.508 _(0.033)	-0.295 _(0.025)
	C.I.	[-0.710, -0.361]	[-0.562, -0.392]	[-0.510, -0.436]	[-0.572, -0.443]	[-0.344, -0.246]
	$\widehat{\gamma}$	0.593 _(0.271)	0.650 _(0.173)	0.279 _(0.130)	1.114 _(0.267)	-0.146 _(0.286)
	C.I.	[0.063, 1.124]	[0.311, 0.989]	[0.025, 0.534]	[0.591, 1.638]	[-0.706, 0.414]
	\widehat{t}_1	-0.471 _(0.429)	-0.774 _(0.336)	-0.889 _(0.131)	-0.674 _(0.193)	-1.328 _(0.352)
	C.I.	[-1.313, 0.370]	[-1.432, -0.116]	[-1.145, -0.632]	[-1.053, -0.295]	[-2.019, -0.638]
	\widehat{t}_2	4.933 _(0.381)	5.378 _(0.180)	5.605 _(0.082)	4.580 _(0.189)	5.389 _(0.269)
	C.I.	[4.186, 5.681]	[5.025, 5.730]	[5.444, 5.766]	[4.209, 4.951]	[4.861, 5.917]

7 Conclusion

In this article, we develop an estimation and inference framework for the multi-kink quantile regression (MKQR) for the longitudinal data. There are also some interesting extension topics. First, since we study the asymptotic normality properties for both estimators given the true number of kink points. However, how to derive the asymptotic properties for estimators under misspecification and make relevant robust inference deserve to be further investigated. Second, different quantile levels may share the same kink points, so it is interesting to investigate the composite estimator for kink points to improve the efficiency. Third, how to extend the proposed method to deal with the missing data is also deserved to be further studied. The inverse probability weighting method (Little and Rubin, 2019) may be helpful. Fourth, we apply the QIF approach to account for the correlation structure. One may consider some other methods to depict the within-subject dependence structures such as copula technique (Wang et al., 2019). We will explore these issues in the future study.

References

- Brumback, B. A. and Rice, J. A. (1998). Smoothing spline models for the analysis of nested and crossed samples of curves. *Journal of the American Statistical Association*, 93(443):961–976.
- Chan, N. H., Yau, C. Y., and Zhang, R.-M. (2014). Group lasso for structural break time series. *Journal of the American Statistical Association*, 109(506):590–599.
- Das, R., Banerjee, M., Nan, B., and Zheng, H. (2016). Fast estimation of regression parameters in a broken-stick model for longitudinal data. *Journal of the American Statistical Association*, 111(515):1132–1143.
- Fan, J. and Zhang, J.-T. (2000). Two-step estimation of functional linear models with applications to longitudinal data. *Journal of the Royal Statistical Society: Series B (Statistical Methodology)*, 62(2):303–322.
- Fryzlewicz, P. et al. (2014). Wild binary segmentation for multiple change-point detection. *Annals of Statistics*, 42(6):2243–2281.
- Ge, X., Peng, Y., and Tu, D. (2020). A threshold linear mixed model for identification of treatment-sensitive subsets in a clinical trial based on longitudinal outcomes and a continuous covariate. *Statistical methods in medical research*, 29(10):2919–2931.
- Hansen, B. E. (2017). Regression kink with an unknown threshold. *Journal of Business & Economic Statistics*, 35(2):228–240.
- Hansen, L. P. (1982). Large sample properties of generalized method of moments estimators. *Econometrica: Journal of the econometric society*, pages 1029–1054.

- Hendricks, W. and Koenker, R. (1992). Hierarchical spline models for conditional quantiles and the demand for electricity. *Journal of the American Statistical Association*, 87(417):58–68.
- Leng, C. and Zhang, W. (2014). Smoothing combined estimating equations in quantile regression for longitudinal data. *Statistics and Computing*, 24(1):123–136.
- Li, C., Dowling, N. M., and Chappell, R. (2015). Quantile regression with a change-point model for longitudinal data: An application to the study of cognitive changes in preclinical alzheimer’s disease. *Biometrics*, 71(3):625–635.
- Li, C., Wei, Y., Chappell, R., and He, X. (2011). Bent line quantile regression with application to an allometric study of land mammals’ speed and mass. *Biometrics*, 67(1):242–249.
- Li, J. and Zhang, W. (2011). A semiparametric threshold model for censored longitudinal data analysis. *Journal of the American Statistical Association*, 106(494):685–696.
- Liang, K.-Y. and Zeger, S. L. (1986). Longitudinal data analysis using generalized linear models. *Biometrika*, 73(1):13–22.
- Little, R. J. and Rubin, D. B. (2019). *Statistical analysis with missing data*. John Wiley & Sons.
- Munro, C. J., Stabenfeldt, G., Cragun, J., Addiego, L., Overstreet, J., and Lasley, B. (1991). Relationship of serum estradiol and progesterone concentrations to the excretion profiles of their major urinary metabolites as measured by enzyme immunoassay and radioimmunoassay. *Clinical chemistry*, 37(6):838–844.
- Qu, A., Lindsay, B. G., and Li, B. (2000). Improving generalised estimating equations using quadratic inference functions. *Biometrika*, 87(4):823–836.
- Qu, Z. (2008). Testing for structural change in regression quantiles. *Journal of Econometrics*, 146(1):170–184.
- Wang, H. J., Feng, X., and Dong, C. (2019). Copula-based quantile regression for longitudinal data. *Statistica Sinica*, 29(1):245–264.
- Wu, H. and Zhang, J.-T. (2002). Local polynomial mixed-effects models for longitudinal data. *Journal of the American Statistical Association*, 97(459):883–897.
- Zhong, W., Wan, C., and Zhang, W. (2021). Estimation and inference for multi-kink quantile regression. *Journal of Business & Economic Statistics*, pages 1–47.